Nuclear Instruments and Methods in Physics Research A 593 (2008) 116–119

Contents lists available at ScienceDirect

Nuclear Instruments and Methods in Physics Research A

journal homepage: www.elsevier.com/locate/nima

Short wavelength regenerative amplifier free electron lasers

D.J. Dunning [a], B.W.J. McNeil [b,*], N.R. Thompson [a]

[a] ASTeC, Daresbury Laboratory, Warrington WA4 4AD, UK
[b] SUPA, University of Strathclyde, Glasgow G4 0NG, UK

ARTICLE INFO

Available online 8 May 2008

PACS:
41.60.Cr

Keywords:
Free electron laser
Regenerative amplifier

ABSTRACT

In this paper we discuss extending the operating wavelength range of tunable Regenerative Amplifier FELs to shorter wavelengths than current design proposals, notably into the XUV regions of the spectrum and beyond where the reflectivity of broadband optics is very low. Simulation studies are presented which demonstrate the development of good temporal coherence in generic systems with a broadband radiation feedback of less than one part in ten thousand.

1. Introduction

A regenerative amplifier free-electron laser (RAFEL) is a high-gain resonator FEL which achieves saturation in a few round-trips of the radiation in a high-loss, and hence low feedback, optical cavity. Because the radiation feedback fraction is low it is feasible that the use of low reflectivity optics in the resonator makes the RAFEL a candidate for short wavelength operation [1]. Several RAFEL proposals have been made in the VUV [2,3] and X-ray [4] and some experimental results obtained [5,6].

There are several expected advantages of the RAFEL over other types of FEL. The RAFEL should be less sensitive to radiation-induced mirror degradation than a low gain oscillator FEL, and the small number of passes required to reach saturation should relax the longitudinal alignment tolerances. The optical feedback also allows the undulator length to be reduced compared to a Self Amplified Spontaneous Emission (SASE) FEL, and it is expected that because of the feedback a RAFEL source can deliver higher quality and more stable pulses than a SASE FEL.

The properties of the transverse modes within the cavity differ from those of a low-gain oscillator FEL. Because of the high loss of the resonator the radiation is not stored over many passes, and because of the high-gain of the FEL the radiation does not propagate freely within the cavity but experiences gain guiding. The cavity's primary function is to return a small field to the start of the undulator to seed the interaction with the subsequent electron bunch. For these reasons it is equally valid to refer to a RAFEL as a High-Gain Self-Seeding Amplifier FEL.

In this paper we present 1D modeling results for a system with a very low feedback factor that returns only $\sim 10^{-5}$ of the undulator output. Such low feedback may occur when mirror reflectivities are very poor, for example into the XUV and X-ray regions of the spectrum. The results are encouraging and suggest that, in principle, a low feedback RAFEL may prove a viable source at these photon energies.

2. A generic high-gain RAFEL

We now consider a generic high gain system shown schematically in Fig. 1 and investigate the properties of such a system when the feedback fraction is reduced to very low levels. First we optimise the feedback fraction using two criteria—the output power and the pulse temporal coherence should both be maximised. We work in the units of the universal scaling [7] where $\bar{z} = z/l_g$ and $l_g = \lambda_w/4\pi\rho$ is the nominal gain length, with λ_w the undulator period and ρ the FEL parameter.

It can be shown from Ref. [8] that the electron beam equivalent shot-noise power is

$$|A_0|^2 \approx \frac{6\sqrt{\pi}\rho}{N_\lambda \sqrt{\ln(N_\lambda/\rho)}} \tag{1}$$

where N_λ is the number of electrons per radiation wavelength. In the exponential gain regime the radiation intensity after a single pass through an undulator of scaled interaction length $\bar{z}$ is then given by

$$|A_1|^2(\bar{z}) \approx \frac{|A_0|^2}{9}\exp(\sqrt{3}\bar{z}) \tag{2}$$

and after returning a fraction F of the output power to the start of the undulator, via some as yet undefined optical system, the seed power at the start of the second pass is $F \times |A_1|^2$. The necessary condition for the development of longitudinal coherence is that this seed power is greater than the shot noise

* Corresponding author. Tel.: +44 141 548 4727.
E-mail address: b.w.j.mcneil@strath.ac.uk (B.W.J. McNeil).

0168-9002/$ - see front matter © 2008 Elsevier B.V. All rights reserved.
doi:10.1016/j.nima.2008.04.045

power, i.e.

$$F \times |A_1|^2 > |A_0|^2.$$

A feedback factor criterion to dominate the shot noise can then be defined as:

$$F_N > 9\exp(-\sqrt{3}\bar{z}). \quad (3)$$

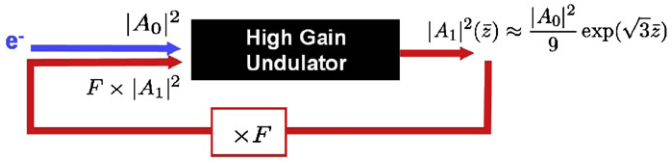

Fig. 1. Schematic representation of a generic high gain RAFEL system.

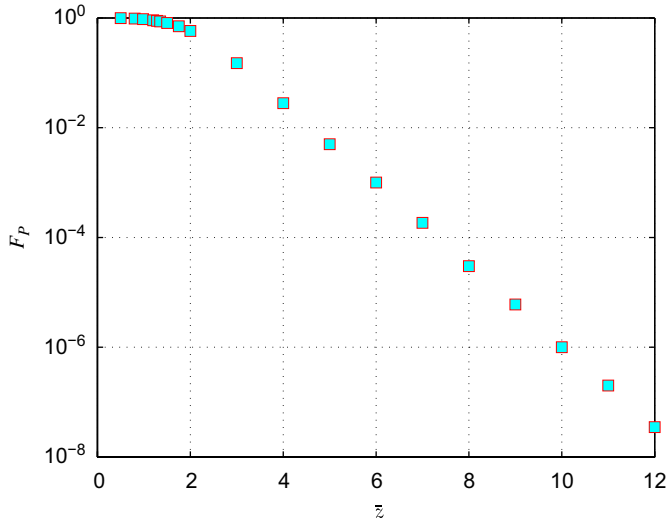

Fig. 2. Results of one-dimensional steady-state simulations to determine the feedback factor F_P that maximises the output power. A fit to the numerical data over the range $3 \leqslant \bar{z} \leqslant 12$, gives $F_P \approx 25\exp(-\sqrt{3}\bar{z})$.

The feedback factor necessary to optimise the output power in the steady state regime only has been determined from 1D simulations, with the results shown in Fig. 2. A fit to the numerical data, valid over the range $3 \leqslant \bar{z} \leqslant 12$, gives

$$F_P \approx 25\exp(-\sqrt{3}\bar{z}). \quad (4)$$

It is seen from comparison of Eqs. (3) and (4) that $F_P \simeq 3F_N$ implying that optimising feedback to maximise the output power will necessarily prove sufficient to dominate the electron beam shot noise and enable the development of coherent pulses. This postulate is tested with 1D time-dependent numerical simulations in the next section.

3. Time dependent simulations

3.1. Simulation method and parameters

We choose a low feedback factor of $F_P = 10^{-5}$ and use Eq. (4) to derive the appropriate scaled interaction length of $\bar{z} = 8.67$. An FEL parameter of $\rho = 2.9 \times 10^{-3}$ is used, typical of XUV FELs, with a peak number of electrons per wavelength of $N_\lambda \approx 3.8 \times 10^5$. The macroscopic profile of the electron bunch is Gaussian, and the input electron beam is monoenergetic. The system is modelled using a 1D time dependent code FELO [9] which solves the 1D FEL propagation equations

$$\frac{d\theta_j}{d\bar{z}} = p_j$$

$$\frac{dp_j}{d\bar{z}} = -(A(\bar{z},\bar{z}_1)\exp[i\theta_j] + \text{c.c.})$$

$$\left(\frac{\partial}{\partial\bar{z}} + \frac{\partial}{\partial\bar{z}_1}\right)A(\bar{z},\bar{z}_1) = \chi(\bar{z}_1)\langle\exp[-i\theta]\rangle \equiv b(\bar{z},\bar{z}_1)$$

where p is the particle energy $p = (\gamma - \gamma_r)/\rho\gamma$ with γ_r the resonant electron energy in units of the electron rest mass, θ the particle phase within the ponderomotive well, $\bar{z}_1$ is the length along the electron bunch from the bunch tail in units of the cooperation

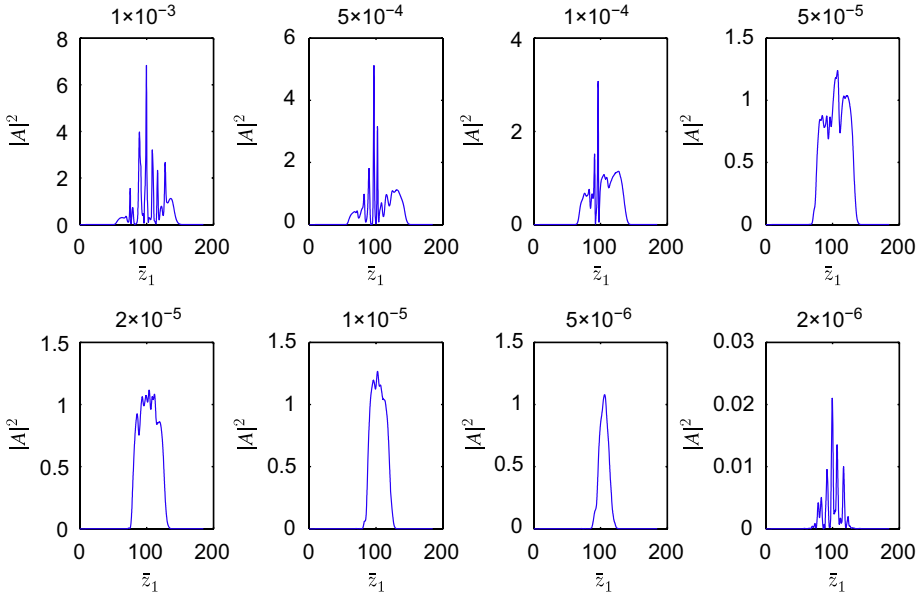

Fig. 3. Typical output pulses of the low feedback RAFEL system. The feedback fraction is shown above each plot, and varies from $F = 1 \times 10^{-3}$ (top left) to $F = 2 \times 10^{-6}$ (bottom right). The cavity detuning value is $\delta_c = 6.0$ for all pulses.

length $l_c = \lambda_r/4\pi\rho$ and $\chi(\bar{z}_1)$ the function describing the macroscopic electron current profile.

The feedback factor was varied from $F = 10^{-3}$ to 2×10^{-6}, and the cavity detuning value δ_c, in units of $\bar{z}_1$, varied from $\delta_c = 0$, defining cavity synchronism, to a detuned cavity length of $\delta_c = 9.0$. For each combination of these parameters the system was allowed to evolve over 200 cavity round trips.

In order to compare the numerical results of the low feedback RAFEL system with a SASE system, 200 separate simulations were done for an equivalent SASE system with $\bar{z} = 14$ where saturation of the pulse energy is seen to occur.

3.2. Simulation results

An analysis has been carried out to determine key parameters of the output pulses pass-by-pass. The parameters of interest are the peak intensity $|A|^2_{\text{peak}}$, the rms pulse length $\sigma_{\bar{z}_1}$, the rms relative linewidth σ_λ/λ and the time bandwidth product $\Delta\nu\Delta t$ which is used to quantify the development of the temporal coherence. The definition used is

$$\Delta\nu\Delta t = \frac{1}{\lambda}\left(\frac{\Delta\lambda}{\lambda}\right)\Delta z \tag{5}$$

with Δz the pulse width. The numerical value obtained depends on the definition of width chosen. The choice used here is $\Delta z = 2\sqrt{2\ln 2} \times \sigma_z$ under which definition a transform limited Gaussian intensity pulse would give the result obtained using FWHM values of $\Delta\nu\Delta t \simeq 0.44$ (the relationship between σ and FWHM for a Gaussian given by $\text{FWHM}(z) = 2\sqrt{2\ln 2} \times \sigma_z$).

3.2.1. SASE results

The results of the SASE simulations are as follows: the root mean square (rms) linewidth over 200 simulations was $\langle\sigma_\lambda/\lambda\rangle = 2.77 \times 10^{-3}$ with an rms pulse length $\langle\sigma_{\bar{z}_1}\rangle = 14.01$ giving a time-bandwidth product of $\langle\Delta\nu\Delta t\rangle = 5.9$. The peak intensity $\langle|A|^2_{\text{peak}}\rangle = 2.2$.

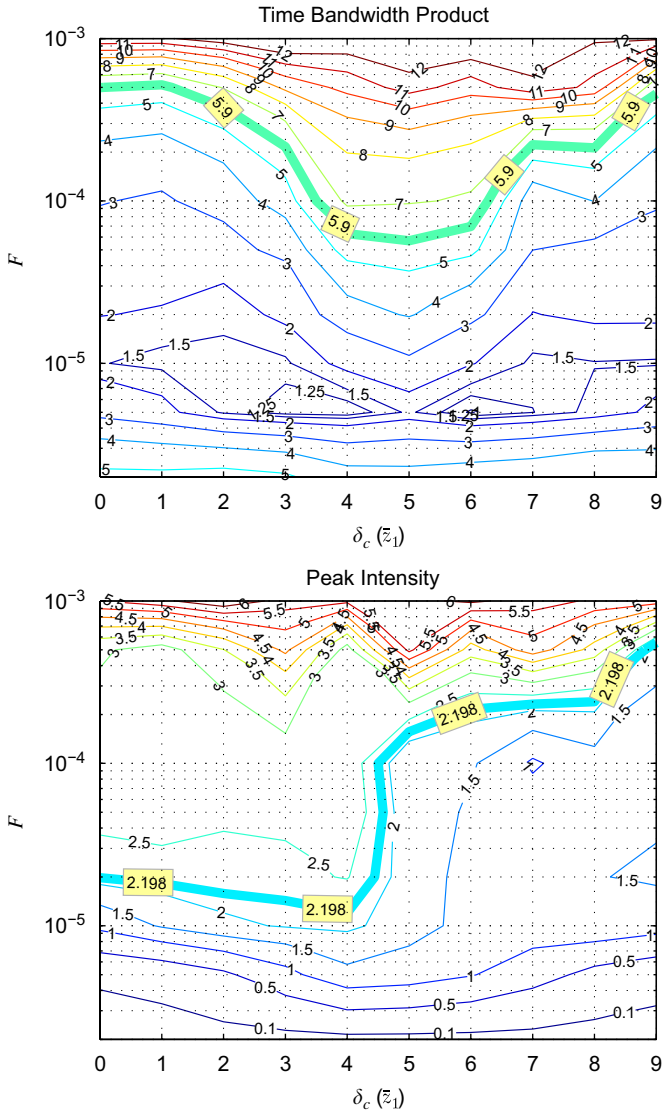

Fig. 4. The complete data for all simulations, in each case averaged over 200 post-saturation pulses, for time-bandwidth product $\langle\Delta\nu\Delta t\rangle$ (top), and peak intensity $\langle|A|^2_{\text{peak}}\rangle$ (bottom). In each plot the vertical axis gives the feedback F and the horizontal axis the cavity detuning δ_c. The bold contour represents the averaged value seen for the 200 SASE simulations.

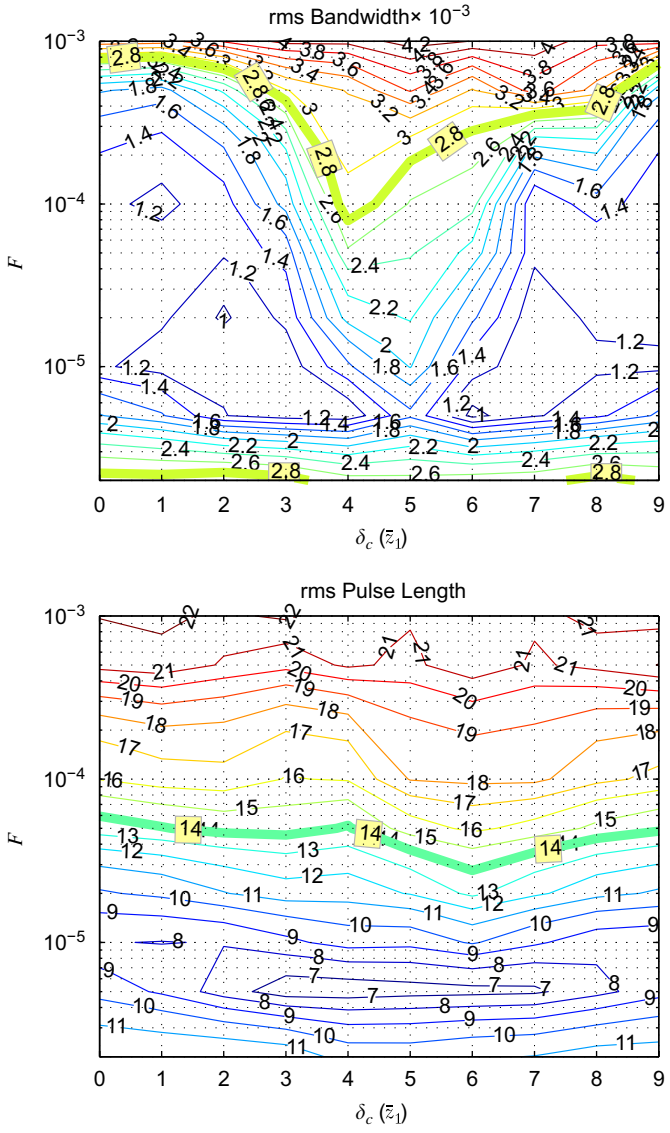

Fig. 5. The complete data for all simulations, in each case averaged over 200 post-saturation pulses, for rms bandwidth $\langle\sigma_\lambda/\lambda\rangle$ (top) and rms pulse length $\langle\sigma_{\bar{z}_1}\rangle$ (bottom). In each plot the vertical axis gives the feedback F and the horizontal axis the cavity detuning δ_c. The bold contour represents the averaged value seen for the 200 SASE simulations.

3.2.2. Low feedback RAFEL results

To identify some features of the RAFEL output, pulse profiles for a feedback fraction decreasing from $F = 10^{-3}$ to 2×10^{-6} are shown first in Fig. 3 for a cavity detuning value of $\delta_c = 6.0$. It is seen that for $F = 10^{-3}$ the pulse profile is spiky with a peak intensity $|A|^2_{\text{peak}} = 7$. The bandwidth for these parameters, averaged over 200 post-saturation passes, is $\langle \sigma_\lambda/\lambda \rangle = 4 \times 10^{-3}$, greater than the mean SASE value of $\langle \sigma_\lambda/\lambda \rangle = 2.77 \times 10^{-3}$, and the time bandwidth product is $\langle \Delta\nu\Delta t \rangle = 12$ compared to the SASE value of $\langle \Delta\nu\Delta t \rangle = 5.9$. These data indicate that the RAFEL pulse is oversaturated. The feedback fraction is too high so that the seed power is too great and the RAFEL saturates before the end of the undulator.

Fig. 3 shows that as the feedback fraction is decreased the pulse profile becomes cleaner, with the front and back of the pulse cleaning up first, leaving a spiky region in the centre of the pulse. This behaviour is attributed to the Gaussian electron current profile—the front and back of the pulse experience less gain and do not oversaturate whereas the centre of the pulse oversaturates. The time bandwidth product falls below the SASE value at a feedback fraction of $F = 5 \times 10^{-5}$. For lower feedback, the time bandwidth product continues to fall until it reaches a minimum value of $\langle \Delta\nu\Delta t \rangle = 1.0$ at a feedback of $F = 5 \times 10^{-6}$. Examination of the pass-by-pass data show individual pulses with $\Delta\nu\Delta t = 0.68$, close to that of a transform limited Gaussian pulse. Finally, as the feedback fraction is reduced further to $F = 2 \times 10^{-6}$ it is seen that there is insufficient feedback for growth to saturation, and the pulse shown represents a pre-saturation SASE pulse for an interaction length $\bar{z} = 8.67$. This conclusion is supported by the fact that the pulse parameters (except peak intensity) have reverted back to close to their values for the SASE simulations.

The complete data for all simulations, in each case averaged over 200 post-saturation pulses, are summarised in the contour plots of Figs. 4 and 5. In each of these plots the vertical axis gives the feedback F and the horizontal axis the cavity detuning δ_c. The bold contour represents the averaged value of the 200 SASE simulations so that, for example, in the top left plot showing time-bandwidth product, the area below the bold contour represents all those feedback and detuning combinations in which the low feedback RAFEL pulses have a lower time-bandwidth product, and hence improved temporal coherence, than the SASE case.

3.3. Discussion of results

It is clear from these simulations that the feedback factor derived in Eq. (4), with a value $F_P = 10^{-5}$ and for interaction length $\bar{z} = 8.67$, is sufficient to significantly improve the temporal coherence of the output compared to SASE, over the full range of cavity detuning values. The feedback corresponding to the best temporal coherence is $F = 5 \times 10^{-6}$ which is a factor of two larger than the criterion derived in Eq. (3) required to dominate shot noise which gives $F_N > 2.7 \times 10^{-6}$.

From examination of the contour plots in Figs. 4 and 5, and considering the previous discussions, three broad regimes can be identified:

- For $F \gtrsim 10^{-4}$: the output has the characteristics of oversaturation;
- For $10^{-4} \gtrsim F \gtrsim 5 \times 10^{-6}$: the applied feedback improves the pulse coherence over SASE;
- For $F \lesssim 5 \times 10^{-6}$: the feedback is insufficient to give growth to saturation or improve the coherence, giving unsaturated SASE output.

4. Conclusion

An overview of the properties of Regenerative Amplifier FELs has been presented and a one-dimensional feasibility study of a generic high-gain RAFEL system which functions using cavity feedback factors as low as 5×10^{-6}. It has been shown that such a system may generate radiation pulses of greatly improved quality than that possible using SASE. The greatest temporal coherence is seen when the power feedback is approximately double the shot noise power. Here the time bandwidth product, averaged over 200 pulses, is $\langle \Delta\nu\Delta t \rangle \approx 1.0$, approximately double that of a transform limited Gaussian pulse. This is more than five times better than the equivalent SASE result, with individual pulses having a time bandwidth product as low as $\Delta\nu\Delta t \approx 0.68$.

It is also seen that if the feedback factor is too high the pulses oversaturate and their properties are similar to, or worse than, the equivalent SASE case.

Methods of attaining the low feedback factors were not discussed, however the fact that they may be so small indicates that there is significant scope in extending the low feedback RAFEL concept into the XUV and possibly further. The possibility of combining harmonic generation methods [10–13] and RAFEL also exists and these exciting possibilities will be the subject of future research.

References

[1] B.W.J. McNeil, IEEE J. Quant. Electron. 26 (1990) 1124.
[2] CCLRC 2006 4GLS Conceptual Design Report Council for the Central Laboratory of the Research Councils (UK) online at ⟨http://www.4gls.ac.uk/documents.htm#CDR⟩.
[3] B.W.J. McNeil, N.R. Thompson, D.J. Dunning, J.G. Karssenberg, P.J.M. van der Slot, K.-J. Boller, New J. Phys. 9 (2007) 239.
[4] Z. Huang, R.D. Ruth, Phys. Rev. Lett. 96 (2006) 144801.
[5] D.C. Nguyen, R.L. Sheffield, C.M. Fortgang, J.C. Goldstein, J.M. Kinross-Wright, N.A. Ebrahim, Nucl. Instr. and Meth. A 429 (1999) 125–130.
[6] B. Faatz, J. Feldhaus, J. Krzywinski, E.L. Saldin, E.A. Schneidmiller, M.V. Yurkov, Nucl. Instr. and Meth. A 429 (1999) 424–428.
[7] R. Bonifacio, C. Pellegrini, L. Narducci, Opt. Commun. 50 (1984) 373–378.
[8] K.J. Kim, Phys. Rev. Lett. 57 (1986) 1871–1874.
[9] B.W.J. McNeil, G.R.M. Robb, D. Dunning, N.R. Thompson, Proceedings of the 28th International Free Electron Laser Conference, Berlin, Germany, 2006, pp. 59-62, Joint Accelerator Conferences Website ⟨http://www.jacow.org⟩.
[10] R. Bonifacio, L. De Salvo Souza, P. Pierini, E.T. Scharlemann, Nucl. Instr. and Meth. A 296 (1990) 787.
[11] L.-H. Yu, Science 289 (2000) 932.
[12] B.W.J. McNeil, G.R.M. Robb, M.W. Poole, N.R. Thompson, Phys. Rev. Lett. 96 (2006) 084801.
[13] B.W.J. McNeil, G.R.M. Robb, M.W. Poole, Phys. Rev. E 70 (2004) 035501 (R).